Cacace, M., Bayer, U., Marotta, A. M. (2008): Strain localization due to structural inhomogeneities in the Central European Basin System. - International Journal of Earth Sciences, 97, 5, 899-913,

DOI: 10.1007/s00531-007-0192-0.

Editorial Manager(tm) for International Journal of Earth Sciences
Manuscript Draft

Manuscript Number:

Title: Strain localization due to structural in-homogeneities in the Central European Basin System

Article Type: Original Paper

Keywords: Central European Basin System; rheological heterogeneities; thin sheet approach; stress and strain localization.

Corresponding Author: Mr Mauro Cacace,

Corresponding Author's Institution: GeoForschungsZentrum Potsdam

First Author: Mauro Cacace, Mr

Order of Authors: Mauro Cacace, Mr; Ulf Bayer; Anna Maria Marotta

Abstract: The large-scale crustal deformations observed in the Central European Basin System (CEBS) are the result of the interplay between several controlling factors, among which lateral rheological heterogeneities play a key role. We present a finite-element integral thin sheet model of stress and strain distribution within the CEBS. Unlike many previous models, this study is based on thermo-mechanical data to quantify the impact of lateral contrasts on the tectonic deformation. Elasto-plastic material behaviour is used for both the mantle and the crust, and the effects of the sedimentary fill are also investigated. The consistency of model results is ensured through comparisons with observed data. The results resemble the present-day dynamics and kinematics when: (1) a weak granite-like lower crust below the Elbe Fault System is modelled in contrast with a stronger lower crust in the area extending north of the Elbe Line throughout the Baltic region; and (2) a transition domain in the upper mantle is considered between the shallow mantle of the Variscan domain and the deep mantle beneath the East European Craton (EEC), extending from the Elbe Line in the south till the Tornquist Zone. The strain localizations observed along these structural contrasts strongly enhance the dominant role played by large structural domains in stiffening the propagation of tectonic deformation and in controlling basin formation and evolution in the CEBS.

Mauro Cacace, Ulf Bayer, Anna Maria Marotta

Strain localization due to structural in-homogeneities in the Central European Basin System

M. Cacace

GeoForschungZentrum (GFZ) Potsdam, Sec. 4.3, Telegrafenberg, 14473 Potsdam, Germany

Tel.: +49-331-2881792

Fax: +49-331-2881349

E-mail: cacace@gfz-potsdam.de

U. Bayer

GeoForschungZentrum (GFZ) Potsdam, Sec. 4.3, Telegrafenberg, 14473 Potsdam, Germany

A. M. Marotta

Department of Earth Sciences, Sec. Geophysics, University of Milan, Milan, Italy

Abstract

The large-scale crustal deformations observed in the Central European Basin System (CEBS) are the result of the interplay between several controlling factors, among which lateral rheological heterogeneities play a key role. We present a finite-element integral thin sheet model of stress and strain distribution within the CEBS. Unlike many previous models, this study is based on thermo-mechanical data to quantify the impact of lateral contrasts on the tectonic deformation. Elasto-plastic material behaviour is used for both the mantle and the crust, and the effects of the sedimentary fill are also investigated. The consistency of model results is ensured through comparisons with observed data. The results resemble the present-day dynamics and kinematics when: (1) a weak granite-like lower crust below the Elbe Fault System is modelled in contrast with a stronger lower crust in the area extending north of the Elbe Line throughout the Baltic region; and (2) a transition domain in the upper mantle is considered between the shallow mantle of the Variscan domain and the deep mantle beneath the East European Craton (EEC), extending from the Elbe Line in the south till the Tornquist Zone. The strain localizations observed along these structural contrasts strongly enhance the dominant role played by large structural domains in

stiffening the propagation of tectonic deformation and in controlling basin formation and evolution in the CEBS.

Keywords: *Central European Basin System, rheological heterogeneities, thin sheet approach, stress and strain localization*

Abbreviations: Central European Basin System (CEBS), Norwegian-Danish Basin (NDB), North German Basin (NGB), Polish Trough (PT), Tornquist Zone (TZ), Sorgenfrey-Tornquist –Zone (STZ), Teysserie-Tornquist-Zone (TTZ), Ringkøbing-Fyn-High (RFH), Elbe Line (EL), Elbe Fault System (EFS), Central Graben (CG), Glüeckstadt Graben (GG), Horn Graben (HG)

Introduction

The Central European Basin System (CEBS) covers a large area from the North Sea to Poland and from Denmark to North Germany. It is composed of two main basins, the Southern Permian Basin and the Northern Permian Basin. These two basins are superimposed on different continental crustal domains with Precambrian to Variscan consolidation ages. The CEBS includes a number of sedimentary sub-basins, among which the major ones are: the Norwegian-Danish Basin (NDB), the North German Basin (NGB), and the Polish Trough (PT) (Fig. 1). The formation and further development of these sub-basins are similar and can be summarized in a three step process (Ziegler 1990; Scheck-Wenderoth and Lamarche 2005): after basins formation in the Late Carboniferous-Early Permian time, accompanied by intense magmatism, a period of thermal subsidence dominated during latest Late Paleozoic and earliest Triassic. The Late Triassic to Late Jurassic evolution was characterized by a rifting phase followed by Cretaceous-Early Cenozoic inversion and a final subsidence stage in the Cenozoic. Studies from different parts of the CEBS (Vejbaek 1997; Berthelsen 1998; Scheck-Wenderoth et al. 2002) have suggested that basin formation and evolution was mainly controlled by the presence of deep reaching zones of lithospheric weakness. Bayer et al. (1997) have related these zones of observed stress and strain localization with the underlying structure of the lower crust or the lithospheric mantle, where areas of reduced viscosity or elevated temperature can play a key role in focusing deformation. In addition, basins evolution was also

strongly influenced by the growth of salt structures (Maystrenko et al. 2005). For example, local salt movements strongly affect and even determine the stress pattern in the overburden (Bayer et al. 1999; Marotta et al. 2000). Moreover, the CEBS is located over a variety of crustal structures which have been tectonically reactivated through time. Dominant are NW-SE striking elements (Fig. 1): (1) the Tornquist Zone (STZ and TTZ) in the north-eastern part of the study area, (2) the Ringkøbing-Fyn-High (RFH), a structural high consisting of faulted blocks separating the Norwegian-Danish Basin from the North German Basin; (3) the Elbe Line (EL) which most probably acts as the southernmost border of the Baltic domain; and (4) the Elbe Fault System (EFS), a weak upper crustal domain active since Late Carboniferous times where strain localization was repeatedly observed and may be ongoing (Mattern 1996; Scheck-Wenderoth et al. 2002). Other important structures are N-S striking grabens which formed during the Mesozoic differentiation phase of the CEBS. The largest of these are the Central Graben (CG), the Glüeckstadt Graben (GG) and the Horn Graben (HG). Due to the superposition of all these distinctive elements, the CEBS shows a very complex structural setting. Regarding basin evolution, new information is now available concerning crustal and shallow mantle structures as derived from gravity modelling (Yegorowa et al. submitted), deep seismic experiments (MONA-LISA Group 1997; DEKORP-BASIN Group 1999), seismic tomography (Gregersen et al. 2002), structural crustal modelling (Gemmer and Nielsen 2001; Scheck-Wenderoth and Lamarche 2005), and stress field modelling (Kaiser et al. 2005). Based on all these results, we used a thin sheet integral modelling approach to investigate the influence of the deep crustal structures and their related rheologies. We tested our results on two different independent observable parameters, the deformation pattern and stress field variations. In order to understand the interconnections between these elements we did not introduce any pre-defined faults in the models like in other studies (Kaiser et al. 2005). However, we relied on previous numerical results in choosing the material parameters and the boundary conditions (Marotta and Sabadini 2003; Marotta et al. 2004; Marotta 2005; Yegorova et al. submitted; Scheck-Wenderoth et al. 2002; Scheck-Wenderoth and Lamarche 2005).

Horizontal deformation velocity field and strain rates

In order to test and quantify the consistency of the numerical model, the obtained results were compared with different types of observable data sets. The first one is the horizontal deformation velocity field. This data set is based on the last ten years of GPS observations which were used to define the ITRF2000 velocity solution database (Altamini et al. 2002). In order to compare the results of our model with geodetic data, the deformation is represented by the horizontal eigenvectors of the strain rate tensor. As already observed in previous work by Marotta (2005), the comparison between the geodetic and the model eigenvalues allows to quantify the quality of the model. Fig. 2 shows the horizontal strain-rate eigenvectors derived from ITRF2000 solutions in Central Europe (black indicating extension, grey compression) computed for triangular domains following the approach of Devoti et al. (2002). The main features are (1) a general SW-NE-directed compression in opposition to a SE-NW-directed extension, and (2) while at high latitudes extension dominates over compression, at middle latitudes the two types of deformation styles are comparable.

Stress field pattern

The second data set used to test the quality of the results is represented by the stress field as obtained from the "World Stress Map Project" (Reinecker et al. 2005). This database provides the direction of the maximum horizontal stress and the related regime as derived from several sources, such as earthquake focal mechanisms, young geological indicators and borehole breakouts (Fig. 3). These data can be compared to the maximum horizontal component of the stress tensor derived from the model. After having obtained the horizontal velocity deformation field, the largest horizontal component of the stress tensor is easily estimated from the horizontal gradients of the velocity field and the nodal values of the viscosity implemented in the thin sheet calculations (Ranalli 1995; Turcotte and Schubert 2002).

Model Set up

A spherical thin sheet approach was adopted to calculate the deformation and the stresses inside the Central European Basin System, based on Marotta et al. (2004) where a detailed description of the mathematical formulation of the method is given. The domain of the CEBS was discretized by 2000 spherical finite triangular elements. Our mesh was obtained by refining of the original grid of Marotta et al. (2004), and then it was adapted to the local frame. The model area covers a region extending from the 50°N to the 60°N parallel and from the 0°E to the 25.5°E meridian. We considered the asthenosphere as an inviscid element thus assuring a stress-free condition at the base of the plate. The lithosphere consists of three main vertical structural layers, the sediments which cover the basin area, the crust (further divided in two layers) and the mantle. Each domain may behave in a brittle, ductile or elastic manner in relation to the thermal state and the local strain rate. For brittle failure plastic deformation is used, therefore all properties depend on pressure but not on temperature or rock type (Byerlee 1978; Cloetingh and Burov 1996). The brittle yield strength, σ_B, follows Byerlee's law (Ranalli 1995; Turcotte and Schubert 2002):

$$\sigma_B = (\sigma_H - \sigma_V)_B = \beta \cdot z \ ;$$

where σ_H and σ_V represent the maximum and the minimum principal stress respectively, z is the depth while β is the brittle failure coefficient depending on the type of fault, the angle of fracture and the pore pressure. Its value amounts 16 MPa·km^{-1} for extensional setting and 40 MPa·km^{-1} for compression (Lynch and Morgan 1987; Jiménez-Munt et al. 2005). For ductile behaviour a power law steady-state flow creep relation is assumed for stresses less than 200 MPa and a typical Dorn law equation for larger stresses (Weertman and Weertman 1975; Ranalli 1995; Turcotte and Schubert 2002). So, the ductile yield strength, σ_D, takes the form:

$$\sigma_D = (\sigma_H - \sigma_V)_D = \left(\frac{\dot{\varepsilon}}{\dot{\varepsilon}_0}\right)^{\frac{1}{n}} \cdot \exp\left(\frac{E}{nRT}\right); \quad \sigma \le 200 MPa$$

$$\sigma_D = \sigma_0 \left\{1 - \sqrt{\left[\left(\frac{RT}{E_A}\right) \cdot \ln\left(\frac{\varepsilon_D}{\dot{\varepsilon}}\right)\right]}\right\}; \quad \sigma \ge 200 MPa$$

where $\dot{\varepsilon}$ is the effective strain rate given by the second invariant of the strain tensor, R is the gas constant, T is the absolute temperature and $\dot{\varepsilon}_0$, n, E, σ_0, E_A and ε_D are material constants depending on the rock type. The yield strength envelope, σ_Y, is given by a contour function assuming the form:

$$\sigma_Y = \pm \min\{|\sigma_B|;|\sigma_D|\},$$

which is positive for extension and negative for compression. The regional strain rate ranges between 10^{-16}-10^{-14} s^{-1} for both compressional and extensional settings (Molnar and Tapponier 1981; Cloetingh and Burov 1996). As demonstrated in previous studies (Lankreijer et al. 1997; Marotta et al. 2000), the results are not strongly affected by changes in strain rate values, because strain rates within one order of magnitude provide changes less than 10%. The effective viscosity (η) is calculated from the depth integral of the yield strength envelope and is a function of the temperature and local strain rate. The boundary conditions imposed on the model are given in terms of crustal thickness and horizontal velocity (Fig. 4a,b). For crustal thickness, the European Moho contour map published by Ziegler and Dèzes (2005) was adapted to the size of the study area and to the nodes of our triangular mesh. For the velocity field, the nodal values of the horizontal velocity obtained from the reference model of Marotta et al. (2004) were adjusted to the new grid. Although different boundary conditions play an important role in terms of stresses and deformations, a detailed analysis of their influences is beyond the purpose of this paper. In order to evaluate the role of the lithospheric structure all calculations were performed with one set of velocity boundary conditions. Neglecting the effects of spreading of the Middle Atlantic Ridge, only the effects related to the counter-clockwise African-Eurasian collision were simulated. Our choice is based on the fact that (1) this type of boundary setting revealed to give the best fit in the reference model of Marotta et al. (2004), and (2) the present-day deformation pattern of the CEBS was mainly caused by collision-induced compressive stresses which followed the Alpine orogeny. The velocity field was then approximated by linear polynomial interpolating functions and numerical integration was performed by Gaussian quadrature with 7 integration points for each element. In relation to the reference model, the modifications can be summarized as follows: (1) we avoided any oversimplification which can limit the capability in reproducing the effects due to variation in crustal and mantle

thickness; (2) lateral contrasts were inserted in the most realistic manner following the information derived from different previous studies; (3) a coupled set of thermo-mechanical equations were used as governing ones.

Crustal and lithospheric mantle thickness variations

In the thin sheet approach the lithosphere is generally treated as one viscous layer or as two layers, mantle and crust, with constant or slightly variable thickness and vertically-averaged rheological properties. Despite the successes reached in reproducing the general stress trend in Europe (e.g. Marotta et al. 2004), the oversimplifications included in these models turned out to be a limit in modelling tectonic scenarios in which depth related processes play an important role. Considering the Moho map (Ziegler and Dèzes 2005), it is evident that the CEBS is characterized by variable crustal thickness ranging from 25 km in its central part down to 48-50 km in the Baltic and East European Craton (EEC). Furthermore, the internal crustal structure is complicated by a thick sequence of sedimentary layers of different age (Ziegler 1990; Bayer et al. 1999; Krawczyk et al. 2002; Scheck-Wenderoth and Lamarche 2005; Majdanski et al. 2006). Going deeper, the asthenosphere-lithosphere thermo-mechanical boundary seems to behave almost similar to the Moho discontinuity, deepening below the EEC domain (Gregersen et al. 2002). As well documented from large seismic experiments (MONA-LOSA Group 1997; DEKORP-BASIN Group 1999) and gravity modelling (Yegorowa et al. submitted), all these features are related to both lateral and vertical changes in geophysical properties. We performed several models for reproducing all the elements described in a stepwise approach in order to quantify their role in deformation.

Lateral rheological contrasts and thermal effects

Lateral structural contrasts have been incorporated in some of the previous models in terms of lateral variations of the Argand number, A_r (England and Houseman 1985; Marotta et al. 2002; Jimènez-Munt et al. 2005). This number provides a measure of the relative importance of viscous and buoyancy forces, and includes the vertically averaged dependence of the viscosity on temperature and lithospheric composition. Its value varies between 0 (for a strong lithosphere) and 50 (for a very soft one), but the parameter is not always consistent with

experimentally observed rock properties (England and Houseman 1989; Jimènez-Munt et al. 2005). Moreover, as widely debated by several authors in the past (England and Houseman 1985; Tomasi et al. 1995; Ranalli 1995) the viscosity has a strong dependence on the temperature profile, which controls the rheology of the Earth. Several studies (Bijwaard et al. 1998; Goes et al. 2000) have demonstrated the presence of 100-300°C fluctuation in the temperature under north-western Europe due to lithospheric mantle thickness variations. This inferred anomalous large scale mantle structure strongly influences the intraplate tectonic activity and may also cause variations in stress and tectonic style. Despite of this fact, most of the previous thin sheet models did not include any thermal calculations or tried to incorporate the temperature-related effects more or less arbitrarily. In order to avoid all these limitations, we implemented a three dimensional thermal conductive model which allows to solve for the temperature field with depth. The most important rock properties, such as radiogenic heat production, thermal conductivity and volumetric expansion coefficient, as derived from several localized studies for the different sub-parts of the study area were also taken into account. The temperature field is then used as input for the rheological model in order to derive the best fit for the CEBS.

Numerical modelling

Many studies in the past have related large-scale deformations to geodynamical causes. The failing in reproducing local features has led to a large number of studies on modes of lithospheric deformation as a function of its rheological structure. We performed several numerical "tectonic deformation experiments" in order to explore the consequences of compositional and thermal parameters. Our goal is the quantification of the impact of rheology on the tectonic deformation and stress setting. Here follows a brief description of the procedure followed and then the main results are discussed.

Case 1: Impact of the sedimentary fill

Model assumptions

To consider the impact of the thermal blanketing of the sedimentary fill, the sediments were modelled as a single vertical layer with a rheology very close to

salt. Table 1 illustrates the model creep parameters, while Fig. 5 shows the sediment thickness map used in all calculations. It was adapted to our study area from the depth-maps published by Scheck-Wenderoth and Lamarche (2005). Its main features can be summarized as follows: there are two directions of depocentre axes, (1) NW-SE-trending with maxima under the Permian Basins and (2) N-S-trending just above the Mesozoic grabens. It images a complex pattern of lows and highs. The basin is framed by the Tornquist Zone in the north and the EFS in the south. The presence of the Ringkøbing-Fyn-High is also represented in the map. In this study case, the other structures comprise a single layered crust overlying a mantle of constant depth of 100 km. The Moho boundary is shown in Fig. 4b. Different models have been performed with creep parameters representing granite, granodiorite, felsic-granulite, diabase and quartzite crustal rocks, while the mantle was imagined with an olivine or a dunite dominated rheology (see Table 1 for the reference parameters).

Results

Despite the differences in rocks properties, the models showed the same general pattern, and therefore we illustrate and discuss only one example. In this case the crust has a quartzite dominated rheology, while the mantle is characterized by olivine creep behaviour, (see Table 2 for the thermal parameters used). Fig. 6 illustrates the results obtained in terms of strain rates and the deformation velocity field. The model resembles the reference deformation pattern shown in Fig. 2. An overall extensional setting oriented mainly NW-SE characterizes the north-eastern part of the domain where almost no sediments are presented, while a compressional deformation style, NE-SW-oriented, becomes comparable to extension or even dominant in the south-west part of the study domain. The inclusion of the sedimentary fill proves to induce higher strain-rate eigenvalues without affecting the deformation style. As major effect the sediments weaken the lithosphere. This is due to their low value of thermal conductivity causing high temperatures in the upper part of the plate (Ziegler et al. 1998; Cloetingh and Van Wees 2005). This weakening effect leads to the formation of wide areas prone for strong deformation, (see Fig. 6) with increased strain rate values in the region covered by sediments.

Case 2: Shallow mantle thermal effects

Model assumptions

For reproducing the shallow mantle discontinuities, the lithosphere was no longer considered as a plate of constant thickness. For modelling the mantle we followed the general results derived from the TOR project (Gregerseen et al. 2002; Voss et al. 2006). This large-scale seismic experiment was mainly concentrated on the deep lithosphere and asthenosphere, confirming the presence of large lateral transitions in the lithosphere of the CEBS. From the TOR results, the transition is considered to be sharp and steep in two places: (1) at the northern rim of the Tornquist Zone near the border between Sweden and Denmark where the lithosphere reaches depths of 200-250 km, and (2) near the southern edge of the Ringkøbing-Fyn-High where the difference becomes smaller, from 90-100 km of depth to 120-150 km. Fig. 7 illustrates the depth map which we generated for the asthenosphere boundary. The parameters used for reproducing the rheology of the sedimentary layer, the crust and the mantle were the same as in Case 1: salt, quartzite and olivine, in order to isolate and quantify shallow mantle thermal effects. The depth map of the asthenosphere, (Fig. 7), illustrates three domains within the study area: (1) a relative weak Variscan domain in the south and south-west; (2) a stiff and strong lithosphere beneath the EEC in the east and north-east, and (3) a transition zone extending between these two areas.

Results

The obtained results reproduce the overall scenario observed after the Late Cretaceous-Early Tertiary Alpine orogeny, when the region between the Sorgenfrey-Tornquist-Zone and the Elbe Line accommodated the main inversion structures, with normal faults being reactivated as reverse faults. The model generates now strong strain localization concentrated along the transition domain (see Fig. 8). The reproduced rheological heterogeneities affect the direction of the strain-rate eigenvectors leading to changes in the azimuth of the eigenvectors. The presence of a stiffer lithosphere below the transitional domain along the asthenosphere boundary acts as a barrier preventing a release of deformation for the area south of it. Coherent with the boundary conditions imposed along the southern border of the domain, compression is mainly NW-SE-directed providing

better agreement with geodetic observations (Fig. 2). Moreover, the results demonstrate that rheological heterogeneities are able to induce changes in the eigenvalues of the strain-rate tensor. As a consequence, the domain between the Elbe Line and the Tornquist Zone is now characterized by higher strain rate eigenvalues. Furthermore, the region of the Polish Trough shows a change in deformation style with a transition from a compressive dominated regime to an extensional one. In order to better constrain the results, the predicted direction of the maximum horizontal stress component, S_{Hmax}, (Fig. 9) was compared with the observed data (Fig. 3). The actual World Stress Map (Reinecker et al. 2005) shows a uniform pattern of WNW-ESE-directed maximum horizontal compressive stress in North Europe with a clockwise rotation toward ENE-WSW in the north-western part of Germany and Poland. The calculated largest horizontal stress field reproduces the fan-like structure only within a limited area. The predicted change in the direction of the largest horizontal stress is localized only in the northeast part of the North German Basin and in the southernmost part of the Polish Trough. The results of Fig. 9 show a mismatch between the predicted and the observed S_{Hmax} in the eastern part of the North Sea. Instead of an observed WNW-ESE-oriented maximum horizontal stress, our results image a NE-SW-oriented S_{Hmax}, almost perpendicular to the observed one. The local mismatch found between the model predictions and the observations may be directly related to the particular composition of the lithosphere in those areas.

Case 3: Lateral rheological heterogeneities in the crust

Model assumptions

In order to reproduce lateral changes in geophysical properties, the crust was split up into two layers. At this point the vertical structures comprise: (1) the sediments with a salt-driven rheology, see Fig. 6 for the depth map; (2) the upper crust with a quartzite or granite rheology and a lower boundary at oscillating depth between 20 and 30 km according to seismic results; (3) a lower crust down to the Moho (Fig. 4b), for which several rheological analogues were implemented; and (4) a mantle of variable thickness (Fig. 8) with an olivine dominated behaviour. As second step, for modelling lateral structural contrasts, we subdivided the whole area into four domains (fig. 10) with different rheologies in the lower crust. Our

choices for the rheological analogues were based on results derived from local studies. The range of P-wave lower crustal velocities (6.2-6.5 km s^{-1}) and densities (2700-2800 kg m^{-3}) observed in the area along the Elbe Fault System motivated a granitic to a granodioritic dominant composition. The high values for P-wave velocities reaching 6.9-7.0 km s^{-1} and the range of densities (2900-3100 kg m^{-3}) in the lower crust north of the Elbe River and below the Sudetes in Poland suggest a lithology typical for gabbros. Finally, we modelled this area with a felsic-granulite composition. To the north this felsic-granulite composed lower crust is bounded by the Tornquist Zone. For the Baltic region we used a slightly stronger mafic-granulite rheology. For the area south of the Elbe Fault system we considered three cases. First the lower crust was modelled with a granodiorite dominant lithology, resembling a weak crustal body. A quartzite composition and a diabase dominated composition were chosen respectively for the second and the third experiments, reproducing a stronger crust. Table 3 summarizes the different data used for the simulations.

Results

We limit the discussion to three examples (Model 2, Model 4 and Model 6 of Table 3) because the best results were obtained by modelling the upper crustal layer with a dominant quartzite rheology. Fig. 11, Fig. 12 and Fig. 13 illustrate the resulting strain rates. Despite of different rheologies used for modelling the Variscan domain, the models generated the same trend, therefore we discuss them together. The main feature shown in the figures is a southward shift of the zone of strain localization. Now, the area with highest deformations is found below the EFS, while a minor compression is still visible along the Tornquist Zone. The lithosphere is weaker beneath the EFS than below the surrounding areas due to the granitic composition in the lower crust which provides increased temperatures. This weakness explains the observed strain localization under this region. The introduction of lateral contrasts improves the results in those locations where the strongest mismatch was found before, maintaining at the same time the overall consistency between the model and observations. The kinematical scenario for the North German Basin is now in agreement with its recent compressional phase and the present- day setting. N-S to NNE-SSW-oriented compression is stronger in the weaker crust below the EFS rather than in the northern part where the predicted

strain rate pattern indicates low deformation rates. This aspect is in agreement with the observed local aseismicity of the region, suggesting a rather undeformable area in the northern part of the basin. The results of Fig. 11, Fig. 12 and Fig. 13 show a change in deformation patterns within the area of the Polish Basin which is now characterized by a N-S-oriented to a NWN-SES-oriented compression. This variation in the deformation patterns indicates that lateral rheological heterogeneities can affect the azimuth of the strain-rate eigenvectors as well as the related eigenvalues. Moreover, the presence of the high-density lower crust below the Polish Trough has moved the centre of maximum strain localization from the TTZ southward. This scenario is in agreement with the present-day tectonic setting of this region which is dominated by a collision-induced compressive intra-continental stress pattern with the main depocentres located in its southernmost part. The predicted orientation of the principal horizontal compressive stress (Fig. 14, Fig. 15 and Fig. 16) shows a general agreement with the present-day stress pattern observed over North Central Europe (Zoback 1992; Reinecker et al. 2005). The modelled stress field images the overall NW-SE-oriented principal axes and also the progressive rotation to S-N/NE in the eastern part of the study region. Focusing on the NGB where many previous studies have failed in predicting the stress field orientation, our results are consistent with the observation showing the fan-like pattern in the direction of S_{Hmax}. Lateral heterogeneities induce changes in the magnitude of the stress tensor as well as in its orientation being able to resemble more local features. Furthermore, the predicted stress regime suggests that the area of the North German Basin and the Polish Trough is still in a state of horizontal compression, having not yet reached isostatic equilibrium as also derived by Marotta et al. (2002). In a regional contest, an overall agreement between the predicted and the observed regional stress field is evident, although there is still a region of mismatch. In fact, the model fails in reproducing the orientation of the S_{Hmax} at its western boundary where it images a NE-SW-oriented maximum stress instead of a NW-SE-oriented one. This can be related to the particular boundary conditions applied along that border, i.e. a pure boundary effect.

Final remarks

A number of models have been presented to test the relative contribution of variations of compositional and thermal parameters to the setting of the regional stress field and deformation pattern in the CEBS. The first sets of models (Case 1 and Case 2) were mainly focused on the evaluation of the effects induced by thermal fluctuations on the predicted stress field and strain pattern. These models resembled the overall features. On the other hand, the introduction of lateral crustal structural heterogeneities is necessary to explain more local features, as shown in Case 3. The presence of lateral contrasts induces changes in the direction of the strain-rate eigenvectors as well as in their related magnitudes. Moreover, lateral rheological heterogeneities affect the direction of the maximum component of the stress tensor. Our results suggest that rheology is a first order driving element for deformations and stresses even in tectonic scenario like the CEBS which are almost dominated by boundary forces.

Conclusions

A viscous thin sheet model has been used to investigate the role of rheological contrasting structures on deformation and stresses focusing on the area of the CEBS. Unlike many previous integral studies, the effects of variations in the thermal regime have been considered in order to determine the best fitting rheologies for different sub-domains. The consistency of the results has been constrained by direct comparisons of the model outcomes and two independent sets of data. For this purpose, the reference parameters are the present-day regional stress field obtained from the "World stress Map Project" (Reinecker et al. 2005) and the strain rate eigenvectors derived by the last ten year GPS observations of the ITRF2000 database (Altamini et al. 2002). The results demonstrate that the observed deformation and stress pattern in the CEBS can be reproduced with reasonable agreement by the model, concerning the overall trend as well as more local features.

Concerning the deformation style, lateral rheological heterogeneities have been proved to induce variations in the azimuth of the strain-rate eigenvectors as already suggested by previous studies (e.g. Marotta 2005). On the other hand, lateral contrasts turn out to affect the strain-rate eigenvalues revealing their key

role in stiffening the propagation of tectonic deformation in the CEBS. In a local contest, the obtained results reproduce a weak lower crust below the EFS and suggest a rather undeformable area in the northern part of the NGB, in agreement with previous results (e.g. Marotta et al. 2000).

In contrast to Golke and Coblentz (1996), we have demonstrated that the direction of the principal stress axes is not totally independent of the rheology of the lithosphere. The presence of different structural domains at crustal and shallow mantle level is responsible for the present-day local variations observed in the direction of the regional stress field. Moreover, our results suggest a present-day state of horizontal compression in the NGB and the PT. This feature is in agreement with previous models (Marotta et al. 2000; Marotta et al. 2002), with results from gravity studies (Scheck-Wenderoth et al. 1999), and with observations from deep seismic experiments (MONA-LISA Group 1997; DEKORP-BASIN Group 1999).

The best agreement between the results and the observations has been found when:

- The sedimentary layer is represented by a salt dominated rheology.
- Variations in the thickness of the lithosphere are modelled, considering a step-wise transition between the Elbe Line in the south and the Tornquist Zone in the north.
- The upper crustal layer is modelled with a stronger quartzite-like rheology rather than with a weaker granite dominated one.
- Lateral structural contrasts at lower crustal depth are considered. These discontinuities comprise the presence of (1) the high density body in the lower crust below north Germany, and (2) a relatively zone of weakness along the EFS.

Our analysis was focused on the influence of large-scale structures on stresses and deformation patterns. It demonstrated that a key factor for the distribution of the compressive stress and strain localization in the CEBS area is the presence of lateral rheological heterogeneities. Strong lateral contrasts are driving the propagation of tectonic deformation and affect the regional tectonic setting.

Acknowledgements:

The authors would like to acknowledge the German Research Council for its financial help, provided within the DFG-SPP 1135 “Dynamics of sedimentary systems under varying stress conditions by example of the Central European Basin System”. We would like to thank Magdalena Scheck-Wenderoth for providing data concerning the sedimentary thicknesses and for her valuable comments. Special thank goes to Yurij Maystrenko for all his help during the first draft of this paper, for providing us with other data set for the calculations and for his constructive review. We are grateful to the Geophysical Institute of Karlsruhe University, especially J. Reinecker, O. Heidbach, M. Tingay, B. Sperner, B. Müller, for providing the WorldStressMap-plots and to Ziegler P.A. and Dèzes P. for their European Moho depth map. All illustrations were made using GMT of Wessel and Smith (1998).

List of references:

Altamini Z, Silard P et al. (2002) ITRF2000: a new release of the International Terrestrial Reference Frame for Earth Science applications. J. Geophys. Res. 107:20001JB000561

Bayer U, Scheck-Wenderoth M et al. (1997) Modelling of the 3D thermal field in the northeast German basin. Geol. Rundsch 86:241-251

Bayer U, Scheck-Wenderoth M et al. (1999) An integrated study of the NE German Basin. Tectonophysics 314:285-307

Beekman F, Bull JM et al. (1996) Crustal fault reactivation facilitating lithospheric folding/buckling in the Central Indian Ocean. Geological Society Special Publication 251-263

Berthelsen A (1998) The Tornquist Zone northwest of the Carpathians: an intraplate pseudosuture. Geol. Stockh. Förh. 120:223-230

Bijwaard H, Spakman W et al. (1998) Closing gap between regional and global travel time tomography. Journ. Geophys. Res. 103:30055-30078

Byerlee JD (1978) Friction of rocks. Pure appl. Geophys. 116:615-626

Christensen NI, Mooney WD (1995) Seismic velocity structure and composition of the continental crust: a global view. Journal of Geophysical Research 100:9761-9788

Chopra P N, Peterson M S (1981) The experimental deformation of Dunite. Tectonophysics 78:453-473.

Cloetingh S, Burov EB (1996) Thermomechanical structure of European continental lithosphere: constraints from rheological profiles and EET estimates. Geophys. J. Int. 124:695-723

Cloetingh S, Van Wees JD (2005) Strength reversal in Europe’s intraplate lithosphere: transition from basin inversion to lithospheric folding. Geology 33:285-288

DEKORP-BASIN Group (1999) Deep crustal structure of the Northeast German Basin: new DEKORP-BASIN’96 deep profiling results. Geology 27:55-58

Devoti R, Ferraro C et al. (2002) Geophysical interpretation of geodetic deformations in the Central Mediterranean area. Tectonophysics 346:151-167

England P, Houseman G (1985) Role of lithospheric strength heterogeneities in the tectonic of Tibet and neighbouring regions. Nature 315:297-301

England P, Houseman G (1989) Extension during continental convergence, with application to the Tibetan Plateau. J. Geophys. Res. 94:17561-17579

Förster A, Förster HJ (2000) Crustal composition and mantle heat flow: implications from surface heat flow and radiogenic production in the Variscan Erzgebirge (Germany). Journal of Geophysical Research 105:27917-27938

Gemmer L, Nielsen SB (2001) Three-dimensional inverse modelling of the thermal structure and implications for lithospheric strength in Denmark and adjacent areas of Northwest Europe. Geophys. J. Int. 147:141-154

Gregersen S, Voss P (2002) Summary of project TOR: delineation of a stepwise, sharp, deep lithosphere transition across Germany-Denmark-Sweden. Tectonophysics 360:61-73

Golke M, Coblentz D (1996) Origins of the European regional stress field. Tectonophysics 266:11-24

Goes S, Loohuis JJP et al. (2000) The effect of plate stresses and shallow mantle temperatures on tectonics of northwestern Europe. Global and Planetary Change 27:23-38

Guterch A, Grad M et al. (1999) POLONAISE'97- an international seismic experiment between Precambrian and Variscan Europe in Poland. Tectonophysics 314:101-121

Hoth K, Rusbült J et al. (1993) Die Tiefen Bohrungen im Zentralabschnitt der Mittleeuropäichen senke-Dokumentation für Geowissenschaften, Berlin

Jimènez-Munt I, Garcia-Castellanos D et al. (2005) Thin-sheet modelling of lithospheric deformation and surface mass transport. Tectonophysics 407:239-255

Kaiser A, Reicherter et al. (2005) Variation of the present-day stress field within the North German Basin- insights from thin shell FE modelling based on residual GPS velocities. Tectonophysics 397:55-72

Kossow D, Krawczyk C et al. (2001) Structural development of the inverted Northeast German Basin. EGU, J. Conf. 6, 337 (ISSN 1362-0886 Cambridge Publications)

Krawczyk C, Eilts F et al. (2002) Seismic evidence of Caledonian deformad crust and uppermost mantle structures in the northern part of the Trans-European Suture Zone, SW Baltic Sea. Tectonophysics 360:215-244

Lamarche J, Scheck-Wenderoth M et al. (2003) Heterogeneous tectonic inversion of the Mid-Polish Trough related to crustal architecture, sedimentary patterns and structural inheritance. Tectonophysics 373:75-92

Lankreijier A, Mocanu V et al. (1997) Lateral variations in lithosphere strength in the Romanian Carpathians: constraints on basin evolution. Tectonophysics 272:269-290

Lockhorst A (1998) NW European Gas Atlas-Composition and Isotope ratios of Natural Gases. Gis application on CD by the British Geological Survey, Bundesanstals für Geowissenschaften und Rohstoffe, Danmarks og Grolnlands Geologiske Undersogelse, Nederlands Instituut voor Toegepaste Geowetenschappen, Panstwowwy Instytut Geologiczny, European Union

Lynch HD, Morgan P (1987) The tensile strength of the lithosphere and the localization of extension. Geol. Soc. Spec. Publ. 28:53-65

Majdanski M, Grad M et al. (2006) 2-D seismic tomographic and ray tracing modelling of the crustal structure across the Sudetes Mountains basing on SUDETES 2003 experiment data. Tectonophysics 413:249-269

Marotta AM, Bayer U et al. (2000) The Legacy of the NE German Basin- reactivation by compressional buckling. Terra Nova 12:132-140

Marotta AM, Bayer U et al. (2002) Origin of the regional stress in the North German basin: results from numerical modelling. Tectonophysics 360:245-264

Marotta AM, Sabadini R (2003) Numerical models of tectonic deformation at the Baltica-Avalonia transition zone during the Paleocene phase of inversion. Tectonophysics 373:25-37

Marotta AM, Mitrovica JX et al. (2004) Combined effects of tectonics and glacial isostatic adjustment on intraplate deformation in central and northern Europe: applications to geodetic baseline analyses. Journal of Geophysical Research 109, B01413

Marotta AM (2005) The fingerprints of intra-continental deformation in Central Europe as envisage by the synergic use of predicting modelling and geodetic data. Bollettino di Geofisica teorica ed applicata 46:181-199

Mattern F (1996) the Elbe Zone at Dresden- a late paleozoic pull-apart intruded shear zone. Z. Dtsch. Geol. Ges. 147:57-80

Maystrenko Y, Bayer U et al. (2005) The Glüeckstadt Graben, a sedimentary record between the North and Baltic Sea in north and central Europe. Tectonophysics, Special Issue 397:113-126

Molnar P, Tapponier P (1981) A possible dependence of the tectonic strength on the age of the crust in Asia. Earth Planet. Sci. Lett. 52:107-114

MONA-LISA Group (1997) the closure of the Tornquist Sea: constraints from MONA LISA deep seismic reflection data. Geology 25:1071-1074

Ranalli G (1995) Rheology of the Earth 2nd ed. Chapman & Hall

Reinecker J, Heidbach O., Tingay M, Sperner B, Müller B (2005) The release 2005 of the World Stress Map. Available online at: www.world-stress-map.org

Roth F, Fleckstein P et al. (1999) Stress orientation found in the NE German differ from the West-European trend. Proceedings of the ICDP/KTB-Kolloquium-BOCHUM 255-264

Scheck-Wenderoth M, Bayer U (1999) Evolution of the Northeast German Basin - inferences from a 3D structural model and subsidence analysis. Tectonophysics 313:145-169

Scheck-Wenderoth M, Bayer U et al. (2002) The Elbe Fault system in North Central Europe-a basement controlled zone of crustal weakness. Tectonophysics 360:281-299

Scheck-Wenderoth M, Lamarche J (2005) Crustal memory and basin evolution in the Central European Basin System-new insights from a 3D structural model. Tectonophysics 297:281-299

Tomasi A, Vauchez A et al. (1995) Initiation and propagation of shear zones in a heterogeneous continental lithosphere. J. Geophys. Res. 100:22083-22101

Turcotte D, Schubert G (2002) Geodynamics 2nd ed. Cambridge University Press

Yegorowa T, Bayer U ET AL: Gravity signals from the lithosphere in the Central European Basin System. Submitted to Tectonophysics

Van Wees JD, Stephenson RA (1995) Quantitative modelling of basin and rheological evolution of the Iberian Basin (Central Spain): implications for lithospheric dynamics of intraplate extension and inversion. Tectonophysics 252:163-178

Van Wees JD, Beekman F (2000) Lithosphere rheology during intraplate basin extension and inversion. Infernces from automated modelling of four basins in western Europe. Tectonophysics 320:219-242

Vejbaek O (1997) Dybe struckturer I danske sedimentaere bassiner. Geol. Tidsskr. 4:1-31

Voss P, Mosegaard K et al. (2006) The Tornquist Zone, a north east inclinig lithospheric transition at the south western margin of the Baltic Shield: revealed through a nonlinear teleseismic tomographic inversion. Tectonophysics 416:151-166

Weertman J, Weertman JR (1975) High temperature creep of rock, and mantle viscosity. Ann. Rev. Earth Planet. Sci. 3:292-315

Ziegler PA (1990) Geological Atlas of Western and Central Europe, 2nd ed. Shell International/Geol. Soc. Publ. House, London, 239 pp.

Ziegler PA, Cloetingh S et al. (1995) Dynamics of intra-plate compressional deformation. Tectonophysics 252:7-59

Ziegler PA, Van Wees JD et al. (1998) Mechanical controls on collision-related compressional intraplate deformation. Tectonophysics 300:103-129

Ziegler PA, Dézes P (2005) Crustal evolution of Western and Central Europe. Memoir of the Geological Society, London

Zoback ML (1992) First-and-second-order patterns of stress in the lithosphere. The World Stress Map Project. Journal of Geophysical Research 97:11703-11728

Figure captions:

Fig. 1 Structural map of the Central European Basin System (Vejabek 1997;Lockhorst 1998; NW European Gas Atlas; Scheck-Wenderoth et al. 2002). The major elements shown are: (1) the Tornquist Zone (TZ) consisting of the Sorgenfrey-Tornquist-Zone (STZ) and the Teysserie-Tornquist-Zone (TTZ). (2) The Ring-köbing-Fyn-High (RFH). (3) The Elbe Fault System (EFS). (4) The N-S-striking Mesozoic Grabens: the Central Graben (CG), the Horn Graben (HG) and the Glueckstadt Graben (GG).

Fig. 2 Triangular horizontal strain-rate eigenvectors derived from the ITRF2000 solutions in Central Europe, (Black indicates extension, and grey compression). The thinner black and grey coloured lines in the left angle indicate non-significant strain rates (modified from Marotta 2005).

Fig. 3 Map showing the direction of the largest horizontal stress for the area under investigation (Reinecker et al. 2005, "The release 2005 of the World Stress Map").

Fig. 4 (a) Finite element grid adopted fort he tectonic predictions in the study.

(b) Crustal thickness variation used in the analysis. Adapted to the domain from the European Moho base-map, Ziegler & Dèzes 2005.

Fig. 5 Map showing the depth of the sedimentary layer used in the thermal and rheological models. It is adapted to the study area from the base-map of the Zechstein published by Scheck-

Wenderoth et al. 2005. The main elements presented are: (1) East European Craton (EEC). (2) Sorgenfrey-Tornquist-Zone (STZ). (3) Teysserie-Tornquist-Zone (TTZ). (4) Polish Trough (PT). (5) Ringkøbing-Fyn-High (RFH). (6) Norwegian-Danish Basin (NDB). (7) Central Graben (CG). (8) Horn Graben (HG). (9) Glueckstadt Graben (GG). (10) North German Basin (NGB). (11) Elbe Fault System (EFS).

Fig. 6 Strain rates (upper figure) and horizontal velocity field (lower figure) obtained only considering the sedimentary thermal blanketing (blue indicates extension, and red compression). There is a general agreement with the reference model depicted in Fig. 2.

Fig. 7 Map showing the lithosphere-asthenosphere isothermal boundary as derived from the TOR experiments results (Gregersen et al. 2002).

Fig. 8 Maximum horizontal strain rate as predicted by the model discussed in Case 2. As a consequence of having considered a transition domain in the lower mantle, the deformation, mainly compression, is now focused along this area.

Fig. 9 Map showing the direction of the maximum horizontal stress component, S_{Hmax}, as predicted by the model discussed in Case 2. The areas framed by dashed quadrates are those where the strongest disagreement was found.

Fig. 10 2-D grid used for the integral model as discussed in Case 3. The lateral domains with different rheological properties in the lower crust are shown.

Fig. 11 Predicted strain-rate eigenvectors for Model 2 of Table 3 (blue stands for extension while red for compression).

Fig. 12 Strain-rate eigenvectors predicted by Model 4 of Table 3.

Fig. 13 Strain-rate eigenvectors obtained from Model 6 of Table 3.

Fig. 14 Predicted direction of the maximum horizontal compressive stress, S_{Hmax}. The illustration refers to the case in which a quartzite-type lower crust was chosen for modelling the domain extending eastward the EFS (Model 2 of Table 3).

Fig. 15 Direction of S_{Hmax} with a felsic-granulite dominated rheology in the lower crust below the eastern part of the study domain (Model 4 of Table 3).

Fig. 16 Predicted S_{Hmax} direction for a granite dominated rheology along the eastern part of the study region (Model 6 of Table 3).

Tables:

Table 1 Creep parameters of the rocks used in the modelling study. (Ranalli 1995; Chopra P N, Peterson M S 1981)

Type of rocks	$\dot{\varepsilon}_0$ ($MPa^{-n} s^{-1}$)	E ($KJ\ mol^{-1}$)	n
Salt	6.3	102	5.3
Quartzite (dry)	6.7×10^{-6}	156	2.4

Diabase (dry)	2.0×10^{-4}	260	3.4
Felsic granulite (dry)	8.0×10^{-3}	243	3.1
Mafic granulite (dry)	1.4×10^{4}	445	4.2
Olivine (dry)	2.4×10^{4}	532	3.5
Dunite (dry)*	6.3×10^{-2}	444	3.41
Granite (dry)	1.8×10^{-9}	123	3.2

Table 2 Values of the parameters used in the thermal modelling (see text for discussion)

Layer	Rheology	Density (kg m^3)	Heat production (W m^{-3})	Thermal conductivity (W m^{-1} K^{-1})
Sediments	Salt	2200	9.7×10^{-7}	2.2
Crust	Quartzite	2850	1.5×10^{-7}	2.5
Mantle	Olivine	3300	0.0	3.4

Table 3 List of models considered in the analysis. The grey colours enlighten the models will be discussed in details.

Layer	**Horizontal subdivision**	**Rheology**	**Model number**
Sediments	None	Salt	1
Upper Crust	None	Granite	
Lower Crust	East-Avalonia	Quartzite	
	High density body	Felsic-Granulite	
	Baltic Shield	Mafic-Granulite	
	EFS	Granite	
Mantle	none	Olivine	
Sediments	None	Salt	2
Upper Crust	None	Quartzite	
Lower Crust	East-Avalonia	Quartzite	
	High density body	Felsic-Granulite	
	Baltic Shield	Mafic-Granulite	
	EFS	Granite	
Mantle	none	Olivine	
Sediments	None	Salt	3
Upper Crust	None	Granite	
Lower Crust	East-Avalonia	Felsic-Granulite	
	High density body	Felsic-Granulite	
	Baltic Shield	Mafic-Granulite	
	EFS	Granite	
Mantle	none	Olivine	
Sediments	None	Salt	4
Upper Crust	None	Quartzite	
Lower Crust	East-Avalonia	Felsic-Granulite	
	High density body	Felsic-Granulite	
	Baltic Shield	Mafic-Granulite	

	EFS	Granite	
Mantle	none	Olivine	
Sediments	None	Salt	5
Upper Crust	None	Granite	
Lower Crust	East-Avalonia	Granite	
	High density body	Felsic-Granulite	
	Baltic Shield	Mafic-Granulite	
	EFS	Granite	
Mantle	none	Olivine	
Sediments	None	Salt	6
Upper Crust	None	Quartzite	
Lower Crust	East-Avalonia	Granite	
	High density body	Felsic-Granulite	
	Baltic Shield	Mafic-Granulite	
	EFS	Granite	
Mantle	none	Olivine	

Figure

Click here to download high resolution image

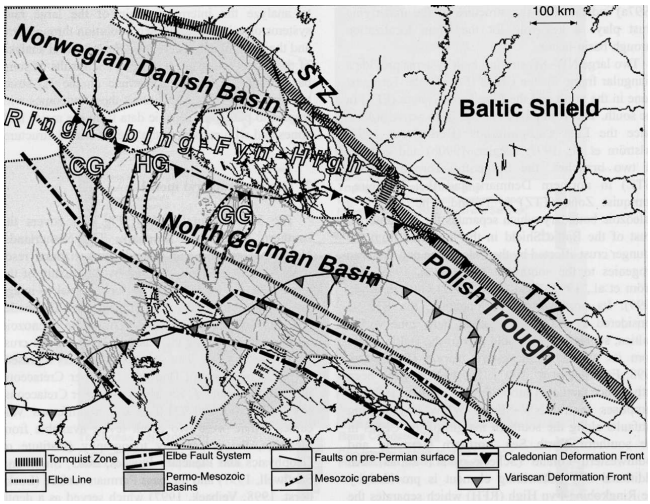

Figure

Click here to download high resolution image

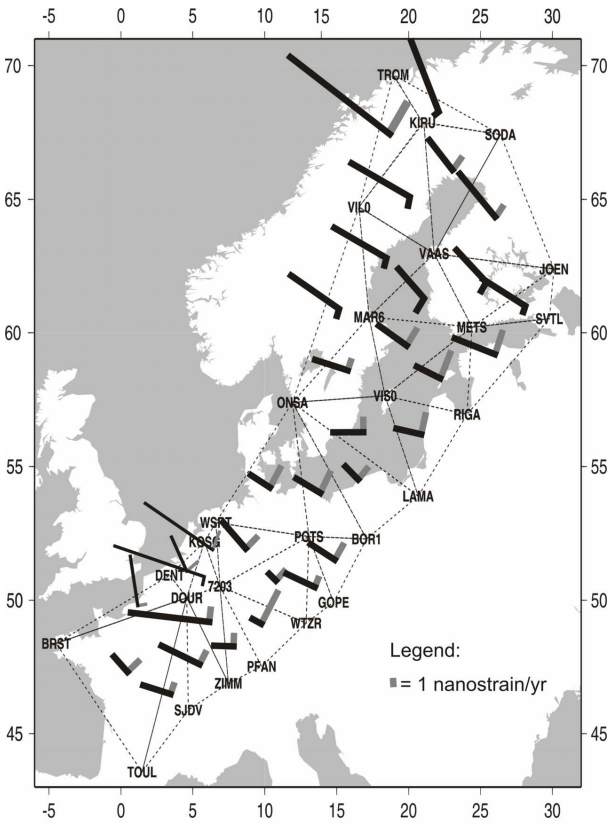

Figure

Click here to download high resolution image

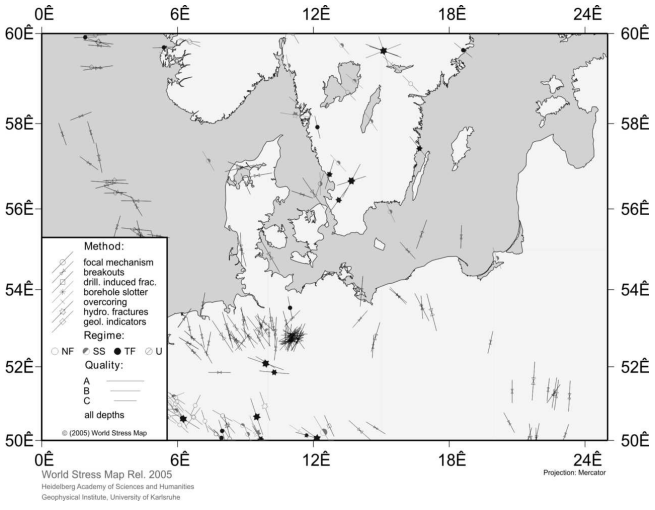

Figure

Click here to download high resolution image

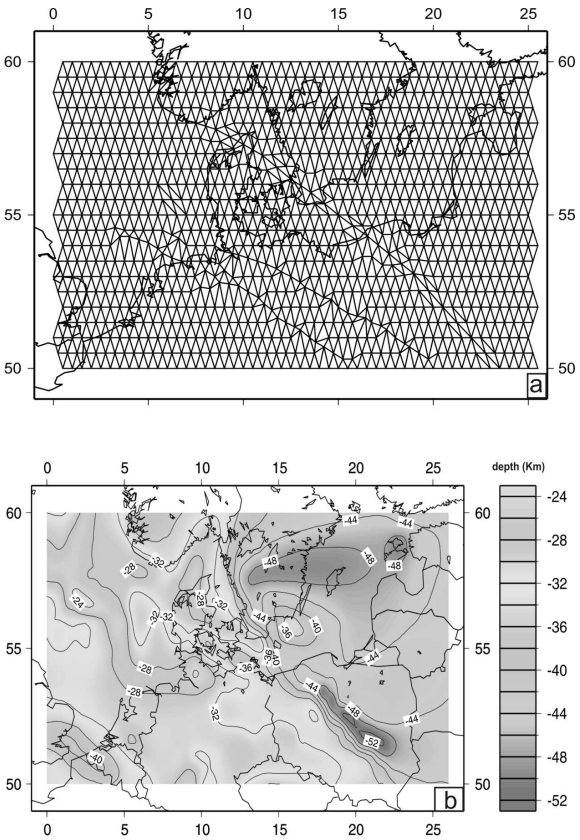

Figure

Click here to download high resolution image

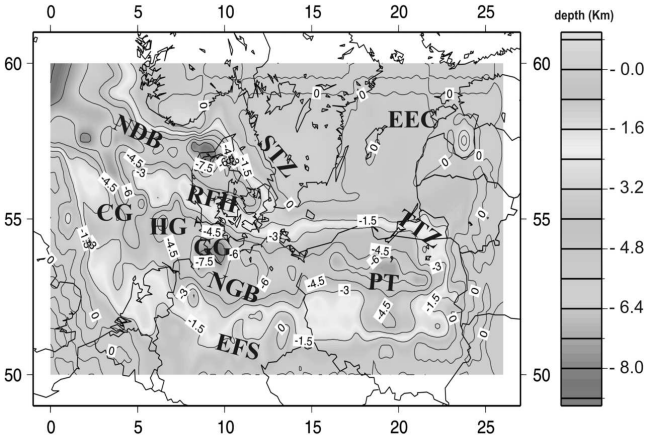

Figure

Click here to download high resolution image

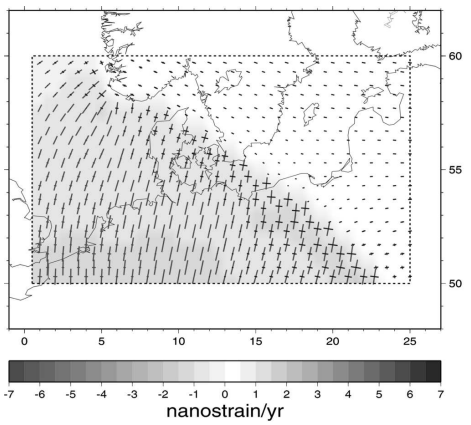

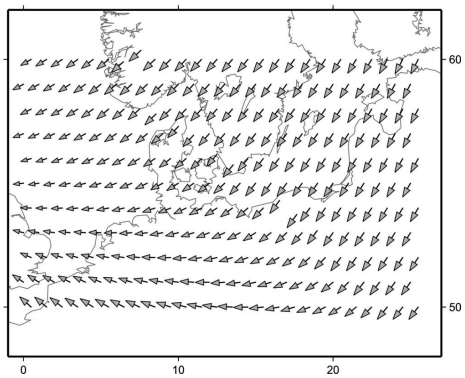

Figure

Click here to download high resolution image

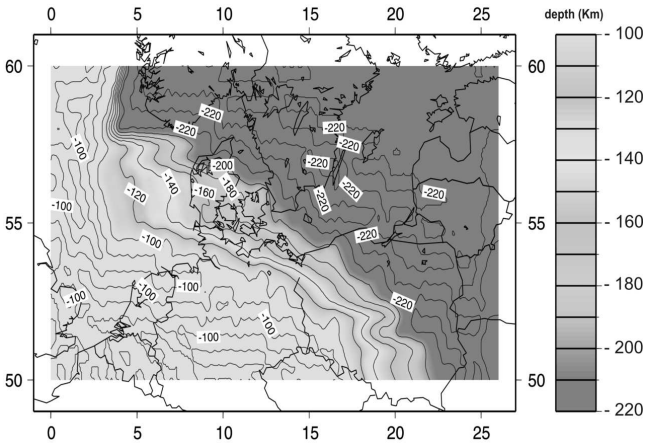

Figure

Click here to download high resolution image

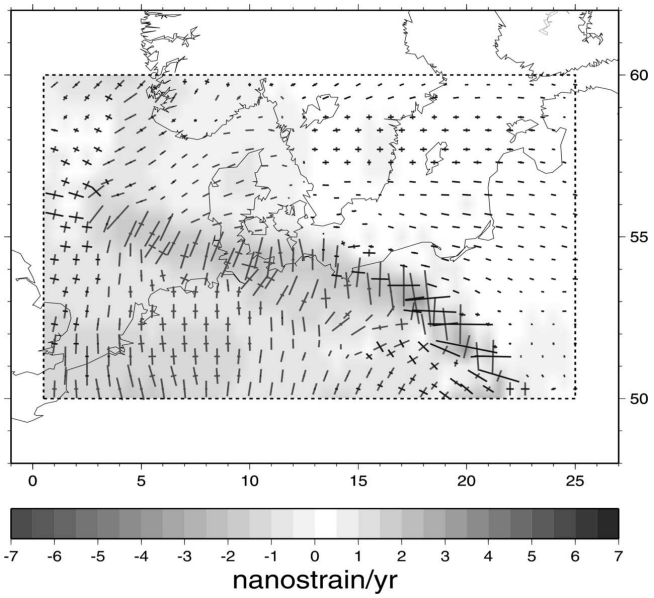

Figure

Click here to download high resolution image

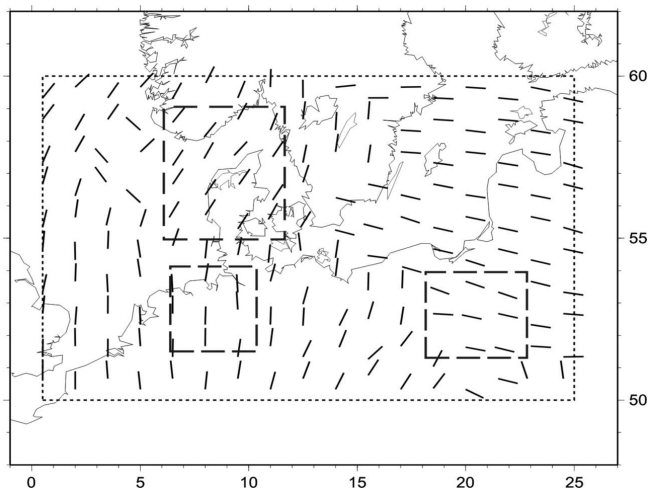

Figure

Click here to download high resolution image

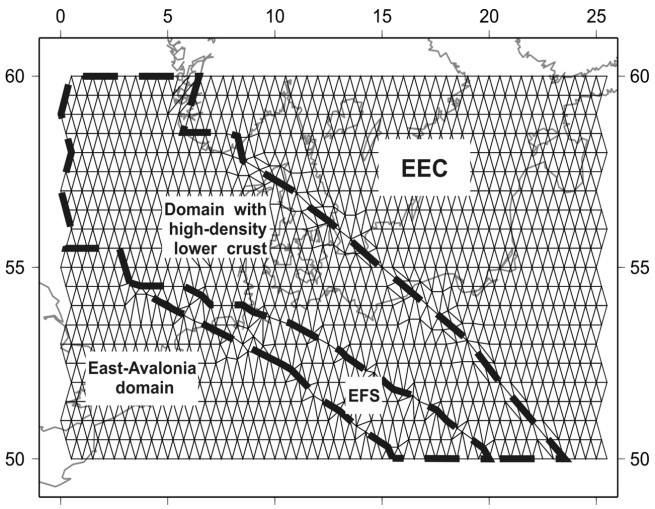

Figure

Click here to download high resolution image

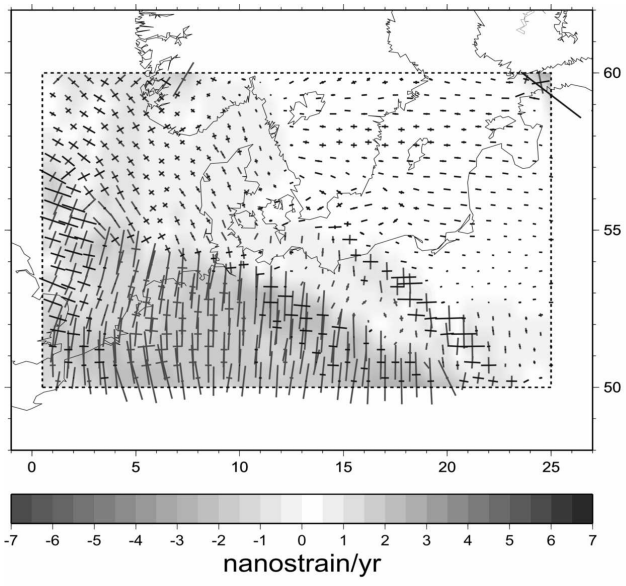

Figure

Click here to download high resolution image

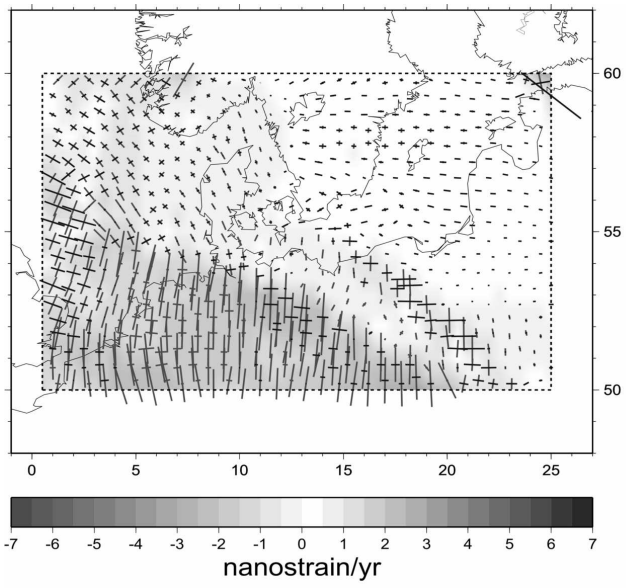

Figure

Click here to download high resolution image

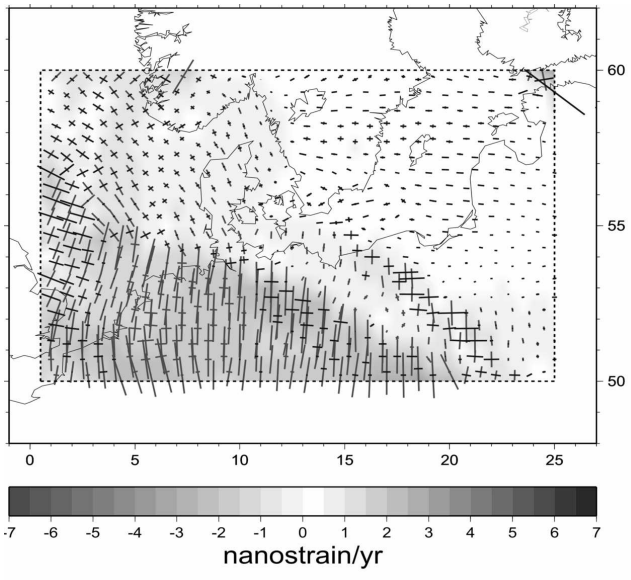

Figure

Click here to download high resolution image

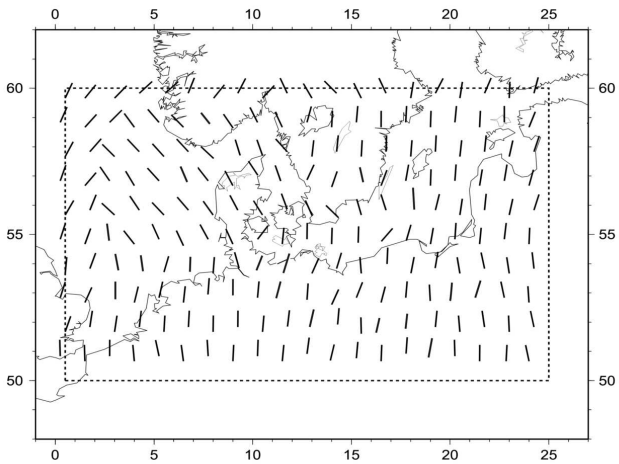

Figure

Click here to download high resolution image

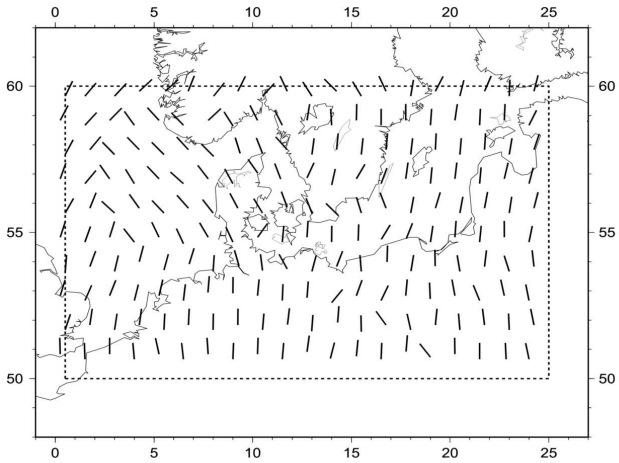

Figure

Click here to download high resolution image

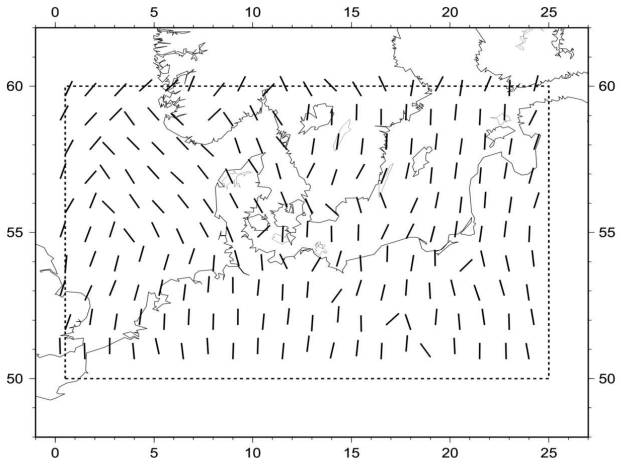

Cover letter

We wish to publish this paper in the special Volume „Dynamics of Sedimentary Basins“, from the EGU session (Wien 2006) under the responsability of the professors Ulf Bayer and Ralf Littke.